JPE 19-5-13

https://doi.org/10.6113/JPE.2019.19.5.1193
ISSN(Print): 1598-2092 / ISSN(Online): 2093-4718

Model-Free Adaptive Integral Backstepping Control for PMSM Drive Systems

Hongmei Li[†,*], Xinyu Li[*,**], Zhiwei Chen[*], Jingkui Mao[*], and Jiandong Huang[*]

[†,*]Department of Electrical Engineering and Automation, Hefei University of Technology, Hefei, China
[**]School of Mechanical and Electrical Engineering, Heze University, Heze, China

Abstract

A SMPMSM drive system is a typical nonlinear system with time-varying parameters and unmodeled dynamics. The speed outer loop and current inner loop control structures are coupled and coexist with various disturbances, which makes the speed control of SMPMSM drive systems challenging. First, an ultra-local model of a PMSM driving system is established online based on the algebraic estimation method of model-free control. Second, based on the backstepping control framework, model-free adaptive integral backstepping (MF-AIB) control is proposed. This scheme is applied to the permanent magnet synchronous motor (PMSM) drive system of an electric vehicle for the first time. The validity of the proposed control scheme is verified by system simulations and experimental results obtained from a SMPMSM drive system bench test.

Key words: Integral backstepping control, Parameter variations, SMPMSM drive system, Ultra-local model, Uncertain disturbances

I. INTRODUCTION

The electric drive system of an electric vehicle is the only source of power for pure electric vehicles. The control quality and operating performance of an electric drive system directly affect the power performance, economy, safety and comfort of electric vehicles [1]. Permanent Magnet Synchronous Motors (PMSM) have the technical advantages of high efficiency, high electromagnetic torque, high power density, low maintenance, and easy realization of high-performance control [2]. Thus, they are widely used in the field of the electric drives of electric vehicles [3].

However, there are many uncertainties and disturbances in the PMSM drive systems of electric vehicles [4]. Specifically, the performance is affected by the cogging torque generated by the interaction between the permanent magnet and the stator core, the harmonic torque caused by the air gap harmonic magnetic field, the nonlinear characteristics of the power switch devices, the inverter nonlinearity due to stray capacitance and the dead time of inverter, the uncertainty of both the electrical parameters and the mechanical parameters caused by different operating conditions, and the external disturbances of the system [5].

A PMSM drive system has used vector control to design the speed and current PI controller to track the speed and current command [6]. The PMSM operated in the Maximum Torque Per Ampere (MTPA) mode when the motor speed was low. When the motor speed increased, the PMSM operated in the field weakening mode. The cascade control structure of the PI speed outer loop and the PI current inner loop is simple and easy to implement. However, it is difficult for linear controllers to implement high-performance current control of nonlinear PMSM drive systems with uncertainties and disturbances [7]. It is difficult to satisfy the technical requirements for achieving the rapidity, steady-state control accuracy and robustness against parameter changes of the electric vehicle PMSM drive systems.

Active Disturbance Rejection Control (ADRC) can make full use of the core control concept of PI control and is a control method of "error eliminating error" [8]. However, this method has some shortcomings such as a large number of parameters to be adjusted, lack of basis for parameter tuning, and lack of practical physical significance of the parameters, which hinder the practical application of ADRC [9].

When compared to ADRC, MFC has the technical advantages of fewer tuning parameters, independence from the controlled

Manuscript received Jun. 26, 2018; accepted Mar. 6, 2019
Recommended for publication by Associate Editor Zheng Wang.
[†]Corresponding Author: hongmei.li@hfut.edu.cn
Tel: +86-0551-62901618, Hefei University of Technology
[*]Dept. of Electr. Eng. and Autom., Hefei Univ. of Technology, China
[**]School of Mechanical and Electrical Eng., Heze Univ., China

system mathematical model, no need for controlled system order information and strong robustness [10]. Therefore, a model-free current control scheme for a PMSM drive system was proposed, which effectively solved the real-time control problems of PMSM drive systems with parametric uncertainties [11]. In order to improve the current control performance of an electric vehicle PMSM drive system, it provides a reference solution.

Backstepping control eliminates the constraint of the relative degree of 1 in the classical design [12]. In addition, it can control real-time n-order nonlinear systems with unmatched uncertainties and unknown parameters. The process of the controller design is systematic and structured. Backstepping control can realize the global stability of a controlled PMSM drive system [13]. However, there are some technical deficiencies such as steady-state control errors and speed overshoot when the load torque changes suddenly [14].

Based on adaptive backstepping control [15] and the Lyapunov stability theory, an original high-order system is equivalently decomposed into several subsystems. Then starting from the low-order subsystem, appropriate state variables are selected as the virtual control variables of the subsystem, and the system control law is designed in reverse step [16]. Adaptive backstepping control is based on less prior knowledge about models and disturbances. Therefore, it is necessary to continuously extract information about disturbances during the operation of the system. The accuracy of the model can be gradually improved.

Adaptive backstepping control has many outstanding advantages [17], [18]. The disturbance uncertainty and parameters uncertainty of a system can be compensated by nonlinear damping or adaptive laws. As a result, adaptive backstepping control has good adaptability and robustness to the disturbance and the parameter uncertainty [19]. For this reason, the study of adaptive backstepping control in the real-time control of PMSM drive systems has gradually gained attention [20]. For example, a PMSM drive system with adaptive backstepping control allows the designer to deal with nonlinearity and uncertainty adaptively in the controller design.

However, adaptive backstepping control still has several deficiencies. For example, the controller design is complex, and the real-time control of a PMSM drive system has a long operation time [21]. Moreover, most adaptive controllers do not guarantee asymptotic convergence of parameter estimates to real values [22].

Considering the technical requirements of fast speed, steady-state control accuracy and robustness against parameter changes of the PMSM drive systems for electric vehicles, this paper innovatively combines adaptive backstepping control [23] with model-free control [24], [25], and proposes a Model-Free Adaptive Integral Backstepping (MF-AIB) control. The design idea is described as follows. First, ultra-local models of the speed loop and the d-q axis current loop are established to estimate the uncertainties and disturbances in real time. Second, starting from the outer loop, appropriate state variables are selected as virtual control variables, and the controller is designed successively in reverse step. On the basis of theoretical research, system simulation and experimental results are combined for a surface-mounted permanent magnet synchronous motor (SMPMSM) drive system to verify the innovation features and feasibility of the proposed MF-AIB control method.

II. SMPMSM System Modeling

In the rotating reference coordinate system, the rotor mechanical angular velocity ω, the d-axis stator current i_d, and the q-axis stator current i_q are selected as state variables. The mathematical model of a SMPMSM can be expressed as follows:

$$\begin{cases} \dot{\omega} = \dfrac{3}{2}\dfrac{p\varphi_f}{J} i_q - \dfrac{B}{J}\omega - \dfrac{T_L}{J} + d_1 \\ \dot{i}_q = -P\omega i_d - \dfrac{R}{L_s} i_q - \dfrac{P\varphi_f \omega}{L_s} + \dfrac{u_q}{L_s} + d_2 \\ \dot{i}_d = -\dfrac{R i_d}{L_s} + P\omega i_q + \dfrac{u_d}{L_s} + d_3 \end{cases} \tag{1}$$

R is the equivalent resistance of the windings. For a SMPMSM, L_s is the inductance of the stator; P is the pole pair number; φ_f is the equivalent magnetic flux of the rotor magnetic field; T_L is the load torque; J is the moment of inertia; and B is the friction coefficient. d_1 represents the disturbance caused by the uncertainty of the mechanical parameters and the unknown disturbance. d_2 and d_3 are expressed as the electrical parameter uncertainty and the disturbance caused by the nonlinearity of the electrical motor on the q and d axes of the stator.

III. Establishing the Ultra-Local Model

For a SMPMSM drive system, three ultra-local models of the outer speed-loop and the inner current-loop of the d-q axis are established:

$$\begin{aligned} \dot{\omega} &= F_\omega + \alpha_\omega i_q^* \\ \dot{i}_q &= F_q + \alpha_q u_q \\ \dot{i}_d &= F_d + \alpha_d u_d \end{aligned} \tag{2}$$

F_ω, F_q and F_d contain unmodeled dynamics and external unknown disturbances in the controlled object, and are continuously updated by the ultra-local model. $\alpha_x \in R$ $(x = \omega, d, q)$ are parameters adjusted by the controller designer [24]. u_d and u_q represent the d-q axis control signals.

For a SMPMSM drive system, comparing equations (1) and (2), the physical variables approached by F_ω, F_q and F_d are:

$$\begin{aligned} F_\omega &= -\frac{B}{J}\omega - \frac{T_L}{J} + d_1 \\ F_q &= -P\omega i_d - \frac{R}{L_s} i_q - \frac{P\varphi_f \omega}{L_s} + d_2 \\ F_d &= -\frac{R i_d}{L_s} + P\omega i_q + d_3 \end{aligned} \tag{3}$$

Using algebraic estimation, accurate estimations of F_ω, F_q and F_d are realized by an inverse Laplace transformation and discretization [11]. The estimate of F_ω is expressed as $\hat{F}_\omega$, and the estimated discrete value of $\hat{F}_\omega[k]$ is expressed as:

$$\begin{aligned} \hat{F}_\omega[k] = &-\frac{3}{n_F^3 T}\sum_{m=1}^{n_F}\Big(\big(n_F - 2(m-1)\big)\times\omega[k-n_F+m-1] \\ &+\alpha_\omega(m-1)T\big(n_F-(m-1)\big)\times i_q[k-n_F+m-3] \\ &+\big(n_F-2m\big)\times\omega[k-n_F+m] \\ &+\alpha_\omega mT\big(n_F-m\big)\times i_q[k-n_F+m-2]\Big) \end{aligned} \tag{4}$$

where T is the control period, the symbol "$[m]$" denotes the value at the (m)th control period, and n_F is the window sequence length.

The estimated discrete value of F_q is expressed as $\hat{F}_q[k]$:

$$\begin{aligned} \hat{F}_q[k] = &-\frac{3}{n_F^3 T}\sum_{m=1}^{n_F}\Big(\big(n_F - 2(m-1)\big)\times i_q[k-n_F+m-1] \\ &+\alpha_q(m-1)T\big(n_F-(m-1)\big)\times u_q[k-n_F+m-3] \\ &+\big(n_F-2m\big)\times i_q[k-n_F+m] \\ &+\alpha_q mT\big(n_F-m\big)\times u_q[k-n_F+m-2]\Big) \end{aligned} \tag{5}$$

The estimated discrete value of F_d is expressed as $\hat{F}_d[k]$:

$$\begin{aligned} \hat{F}_d[k] = &-\frac{3}{n_F^3 T}\sum_{m=1}^{n_F}\Big(\big(n_F - 2(m-1)\big)\times i_d[k-n_F+m-1] \\ &+\alpha_d(m-1)T\big(n_F-(m-1)\big)\times u_d[k-n_F+m-3] \\ &+\big(n_F-2m\big)\times i_d[k-n_F+m] \\ &+\alpha_d mT\big(n_F-m\big)\times u_d[k-n_F+m-2]\Big) \end{aligned} \tag{6}$$

IV. Model-Free Adaptive Integral Backstepping Control

The MF-AIB technique is mainly based on the stability of the Lyapunov function. This algorithm is used for the current loop and speed loop control of an EV permanent magnet synchronous motor drive system.

A. MF-AIB Virtual Control of the Speed Loop

The dynamic error between the rotor mechanical angular velocity ω and the reference value ω^* is defined as:

$$e_\omega = \omega^* - \omega \tag{7}$$

By using the operation of the derivative for the error and substituting an ultra-local model into the speed loop, the derivative of the rotor mechanical angular velocity tracking error can be deduced as follows:

$$\begin{aligned} \dot{e}_\omega &= \dot{\omega}^* - \dot{\omega} \\ &= \dot{\omega}^* - F_\omega - \alpha_\omega i_q \end{aligned} \tag{8}$$

To ensure the stability of the nonlinear system and that the error converges to zero, the Lyapunov function $V_1(e_\omega)$ is set to be a global positive definite.

$$V_1(e_\omega) = \frac{1}{2}e_\omega^2 \tag{9}$$

The derivative of the Lyapunov function $V_1(e_\omega)$ is:

$$\begin{aligned} \dot{V}_1(e_\omega) &= e_\omega \dot{e}_\omega \\ &= e_\omega(\dot{\omega}^* - \alpha_\omega i_q - F_\omega) \end{aligned} \tag{10}$$

If the derivative of the Lyapunov function is a semi-negative definite, that is, $\dot{V}_1(e_\omega) = -k_1 e_\omega^2 \le 0$ ($k_1 > 0$), the error converges to zero.

$$\dot{V}_1(e_\omega) = e_\omega(\dot{\omega}^* - \alpha_\omega i_q - \hat{F}_\omega) = -k_1 e_\omega^2 \tag{11}$$

According to formula (11), the reference value of the stator q-axis current is generated, and the following formula is obtained:

$$i_q^* = \frac{1}{\alpha_\omega}(k_1 e_\omega + \dot{\omega}^* - \hat{F}_\omega) \tag{12}$$

The proportion term can only be used to accelerate convergence. By adding an integral term, the steady-state error caused by modelling deviations and system uncertainty can be eliminated while achieving a fast convergence. To this end, formula (12) is rewritten to:

$$i_q^* = \frac{1}{\alpha_\omega}(k_1 e_\omega + k_4\int e_\omega + \dot{\omega}^* - \hat{F}_\omega) \tag{13}$$

B. MF-AIB of the q-Axis Current Loop

The dynamic error between the actual state value i_q and the reference value i_q^* of the stator is defined as:

$$e_q = i_q^* - i_q \tag{14}$$

The derivative of the stator q-axis current tracking error can be derived by substituting the ultra-local model into the derivative of the q-axis current.

$$\begin{aligned} \dot{e}_q &= \dot{i}_q^* - \dot{i}_q \\ &= \dot{i}_q^* - F_q - \alpha_q u_q \end{aligned} \tag{15}$$

In order to ensure the stability of the stator quadrature current and the error convergence to zero, the Lyapunov function $V_2(e_q)$ is set to be a global positive definite.

$$V_2\left(e_q\right)=\frac{1}{2}e_q^2 \tag{16}$$

The derivative of $V_2\left(e_q\right)$ is:

$$\begin{aligned}\dot{V}_2\left(e_q\right)&=e_q\dot{e}_q\\&=e_q(\dot{i}_q^*-F_q-\alpha_q u_q)\end{aligned} \tag{17}$$

If the derivative of the Lyapunov function is a semi-negative definite, that is, $\dot{V}_2\left(e_q\right)=-k_2e_q^2\le 0$ ($k_2>0$), the error converges to zero.

$$\dot{V}_2\left(e_q\right)=e_q(\dot{i}_q^*-\hat{F}_q-\alpha_q u_q)=-k_2e_q^2 \tag{18}$$

According to formula (18), the control law of u_q is designed as follows:

$$u_q=\frac{1}{\alpha_q}(k_2e_q+\dot{i}_q^*-\hat{F}_q) \tag{19}$$

C. MF-AIB of the d-Axis Current Loop

In order to realize complete decoupling and accurate current tracking of a PMSM controller, the current reference value can be made as follows:

$$i_d^*=0 \tag{20}$$

The tracking error between the reference value i_d^* and the state value i_d of the stator is defined as:

$$e_d=i_d^*-i_d \tag{21}$$

The derivative of the stator d-axis current tracking error can be derived by substituting the ultra-local model into the derivative of the d-axis current.

$$\begin{aligned}\dot{e}_d&=\dot{i}_d^*-\dot{i}_d\\&=\dot{i}_d^*-F_d-\alpha_d u_d\end{aligned} \tag{22}$$

In order to ensure the stability of the stator d-axis current and the convergence error to zero, the Lyapunov function $V_3\left(e_d\right)$ is set to be a global positive definite.

$$V_3\left(e_d\right)=\frac{1}{2}e_d^2 \tag{23}$$

The derivative of the Lyapunov function $V_3\left(e_d\right)$ is:

$$\dot{V}_3\left(e_d\right)=e_d\dot{e}_d=e_d(\dot{i}_d^*-F_d-\alpha_d u_d) \tag{24}$$

If the derivative of the Lyapunov function is a semi-negative definite, that is, $\dot{V}_3\left(e_d\right)=-k_3e_d^2\le 0$ ($k_3>0$), the error converges to zero.

$$\dot{V}_3\left(e_d\right)=e_d(\dot{i}_d^*-\hat{F}_d-\alpha_d u_d)=-k_3e_d^2 \tag{25}$$

According to Formula (25), the control law of u_d is designed as follows:

$$u_d=\frac{1}{\alpha_d}(k_3e_d+\dot{i}_d^*-\hat{F}_d) \tag{26}$$

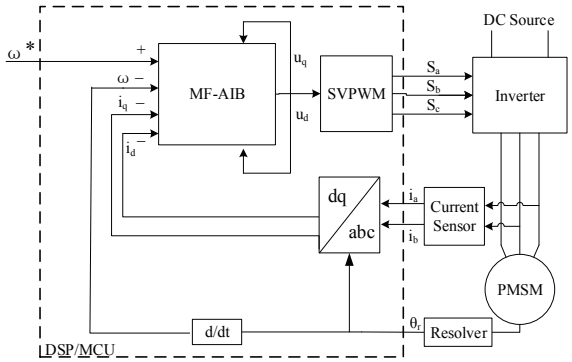

Fig. 1. Structural block diagram of a SMPMSM drive system controlled by the model-free adaptive integral backstepping (MF-AIB) control.

TABLE I
MOTOR SPECIFICATIONS

Parameters	Values
Stator resistance R	0.0957Ω
Stator inductance L_s	1mH
Moment of inertia J	0.01015
Friction coefficient B	0.01
Number of pole-pairs P	12
Magnet flux φ_f	0.027Wb
Rated current I_r	27Arms
Rated torque T_r	13N·m

A control block diagram of the model-free adaptive integral backstepping (MF-AIB) control for a PMSM drive system is shown in Fig. 1. θ_r is the rotor position angle measured by a resolver and the stator current is measured by a LEM LA25-P Hall effect current sensor.

V. SYSTEM SIMULATION

In the MATLAB/Simulink environment, a PMSM driving system controlled by the MF-AIB is simulated and compared with PI control under the same conditions. The motor parameters are shown in Table I. Considering the influence of the dead-time of the inverter, the dead-time of the inverter is set to 2μs.

The current loop PI regulator parameter tuning method has been studied in a large number of literatures. There is no uncertainty compensation scheme in traditional PI control. It can only be a tradeoff between a fast response and an overshoot to obtain the PI control parameters [26]. The bandwidth ω_b of the PI current loop is set to 400Hz (2512rad/s). Based on this, the d-q axis control parameters (parallel PI controller) are selected [27] as:

$K_p=\omega_b L_s=2.51$, $K_i=\omega_b R_s=240.52$.

The parameters $K_{p\omega}$ and $K_{i\omega}$ of the PI regulator in the outer loop of a SMPMSM drive system can be adjusted by

TABLE II
CONTROL PARAMETERS OF THE PI

Control parameters	Values
Speed loop $K_{P\omega}$	$K_{P\omega}=2.057$
Speed loop $K_{i\omega}$	$K_{i\omega}=206$
d-axis current loop K_{Pd}	$K_{Pd}=2.51$
d-axis current loop K_{id}	$K_{id}=241$
q-axis current loop K_{Pq}	$K_{Pq}=2.51$
q-axis current loop K_{iq}	$K_{iq}=241$

TABLE III
CONTROL PARAMETERS OF THE MF-AIB

Control parameters	Values
MFC coefficient α_{dq}	$\alpha_{dq}=750$
MFC coefficient α_{ω}	$\alpha_{\omega}=668$
Speed gain k_1	$k_1=174.88$
q Gain k_2	$k_2=2250$
d Gain k_3	$k_3=2250$
Speed gain k_4	$k_4=0.017$

the following formula [28]:

$$\begin{cases} K_{p\omega}=\dfrac{\beta J}{1.5P_n\varphi_f} \\ K_{i\omega}=\beta K_{p\omega} \end{cases} \tag{27}$$

β is the desired bandwidth of the speed loop. Bandwidth is the only tuning factor when the PI parameters are adjusted. For a comprehensive performance comparison, β=100rad/s is chosen. Then $K_{p\omega}=2.057$ and $K_{i\omega}=206$. The PI control parameters are shown in Table II.

The proposed MF-AIB uses the pole configuration technique to tune its control parameters [29]. On the one hand, a broader bandwidth corresponds to better tracking performance, interference suppression performance and sensitivity to parameter changes. On the other hand, the bandwidth is easily limited by sensor noise and dynamic uncertainty. For the sake of simplicity and practicality, only the bandwidth ω_c is chosen as the measure of control performance, and ω_c is the cut-off frequency.

The poles are placed in $-\omega_c$. Both practicality and simplicity show that ω_c is the only adjustable control parameter using pole configuration technology, which can greatly simplify the process of setting the control parameters and guarantee the control performance. The MF-AIB is designed as a critical velocity response. Table III lists the MF-AIB control parameters.

Firstly, the speed response of a SMPMSM driving system at no-load starting under a given load torque is simulated. Then the proposed control and PI control are compared by simulation. As shown in Fig. 2(a), the given load torque varies

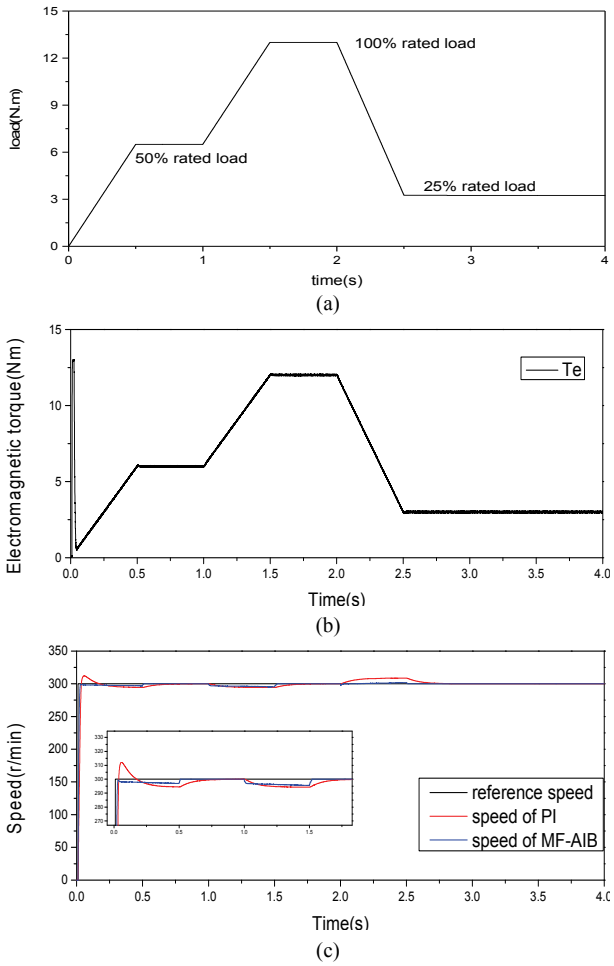

Fig. 2. Comparison of the proposed controller and a PI controller in case of a load slope change. (a) Given load torque. (b) Torque response of the proposed scheme. (c) Comparison of the speed response between the proposed control and PI control.

with increases and decreases in the slope. Fig. 2(b) shows the electromagnetic torque tracking curve of the proposed controller. By comparing Fig. 2(a) with Fig. 2(b), it can be verified that the MF-AIB has good torque tracking capability. A speed comparison between the proposed controller and the PI controller is shown in Fig. 2(c). The motor runs at a speed of 300r/min. The given load changes, as shown in Fig. 2(a), which affects the speed of the motor rotor. These simulation results show that, when compared with a PI controller, the proposed controller has stronger load disturbance rejection capability and less overshoot/undershoot speed.

Secondly, a simulation study of the speed tracking control performance of a SMPMSM driving system under no-load starting is carried out. The rotor speed curve is designed to include a combination of rising slope and falling slope. The obtained response results of the MF-AIB and PI control simulations are shown in Fig. 3. The MF-AIB (represented by the red curve) has a very strong speed tracking ability and almost coincides with the given curve. Meanwhile, the PI control (represented by the blue line) has a tracking delay in

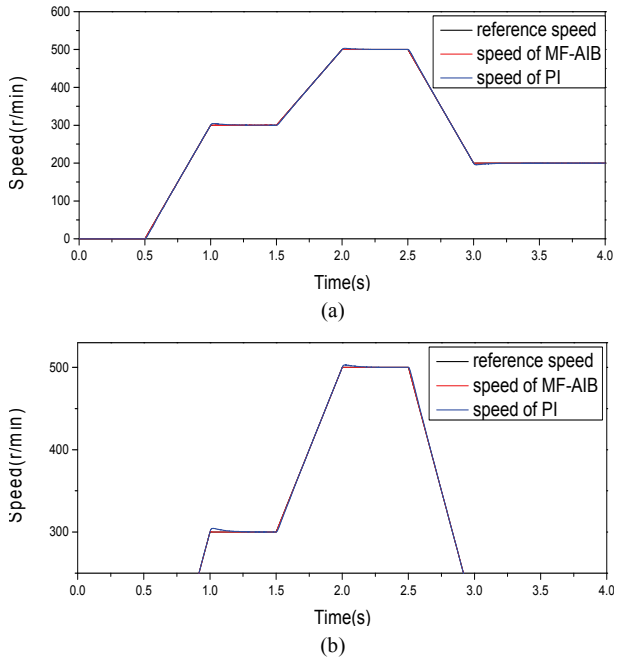

Fig. 3. Speed response of the proposed control and PI control at a given slope speed. (a) Slope speed tracking characteristics. (b) Local chart of the slope speed tracking characteristics.

the slope tracking state, and PI overshoot occurs when the speed operation mode is switched.

In order to verify the load disturbance rejection capability of the MF-AIB and to demonstrate the superiority of the disturbance estimation, simulations while suddenly applying load torque during stable operation are carried out. In this simulation, the PMSM gives a 300r/min step speed instruction at 0.01 seconds, and the motor torque increases from 0 to 5N.m at 0.5 seconds. Fig. 4(a) shows a speed comparison between the MF-AIB control and PI control. The speed step response of the proposed control method does not have an overshoot, and the speed can be quickly restored to a given value after a sudden increase of the load torque. Fig. 4(b) shows the d-axis current disturbance estimation curve ($\hat{F}_d$) and the q-axis current disturbance estimation curve ($\hat{F}_q$) estimated by the ultra-local model.

No clutter or white noise is introduced in the simulation, and the illustrated disturbance is mainly caused by load torque. The curve shown in Fig. 4(c) is the estimated uncertain disturbance, which affects the motor speed. The d-q axis current generated by the MF-AIB is shown in Fig. 4(d), and the current waveform is stable in the steady state. Fig. 4(e) shows that the MF-AIB control at 0.5s produces a larger q-axis current than PI control, which generates a larger electromagnetic torque to offset the load torque, and drives the motor rotor to maintain the given speed. Finally, the good load disturbance rejection capability of the proposed control method is verified.

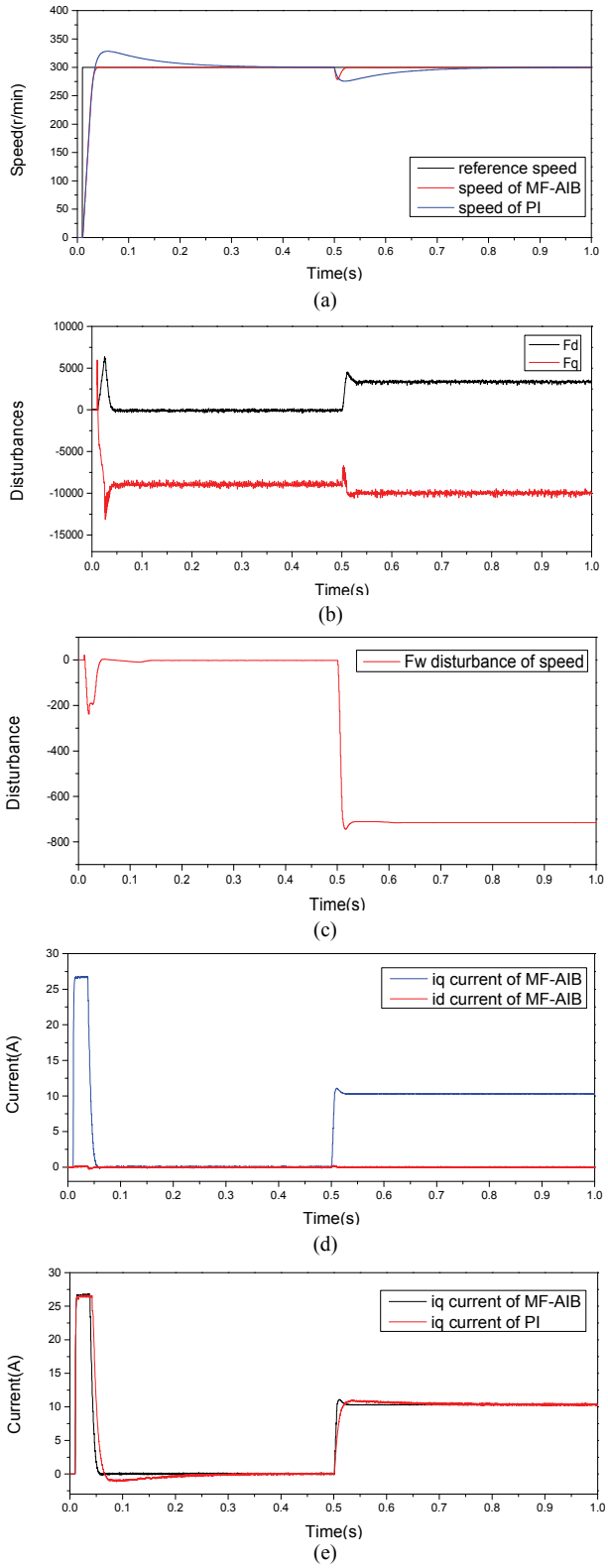

Fig. 4. Response of the MF-AIB under a 5N.m step-load when operating at 300r/min. (a) Speed performance comparison between the MF-AIB control and PI control. (b) Current loop disturbance estimated by the MF-AIB. (c) Rotor velocity disturbance estimated by the MF-AIB. (d) d-axis and q-axis currents of the MF-AIB. (e) q-axis current comparison between the MF-AIB control and PI control.

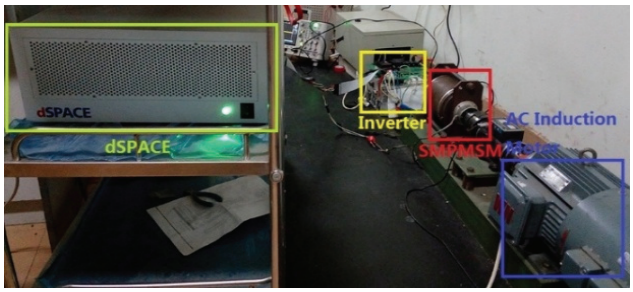

Fig. 5. Experimental bench of a SMPMSM drive system.

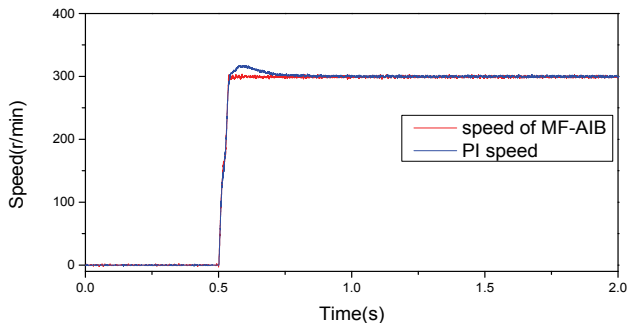

Fig. 6. Speed step response of the MF-AIB control and PI control under no-load conditions.

VI. Experimental Results

In order to verify the speed tracking capability and the load disturbance rejection capability of the MF-AIB, a number of bench experiments are carried out for a 900W PMSM.

Fig. 5 shows the drive system of an electric vehicle controlled by the MF-AIB, including an AC induction motor, control interface, power board, inverter, PMSM, dynamometer and dSPACE platform.

In the test bench, the SMPMSM is connected to a 2.2kW AC induction dynamometer and driven by a MOSFET module inverter. The dead time of the inverter is set to 2μs, using a DS5202 and a dSPACE/DS1007 as the inverter controller. The rotor position is measured by a resolver and the stator current is measured by a LEM LA25-P Hall effect current sensor. The d-q axis current is transmitted by dSPACE and Control Desk, and the phase current is measured by the oscilloscope's current probe. The asynchronous motor drive system operates in the torque control mode, while the tested SMPMSM drive system operates in the speed control mode. Table I gives the nominal parameters of the motor. The control coefficients of the two control algorithms are shown in Table II and Table III.

In order to validate the starting performance of the PMSM under no-load conditions, the speed step control characteristics of the MF-AIB control and PI control are compared experimentally. At 0.5s, the proposed controller and PI controller drive the rotor speed from 0 to 300r/min.

A mathematical model of the internal disturbance and its external environment for the controlled object has not been

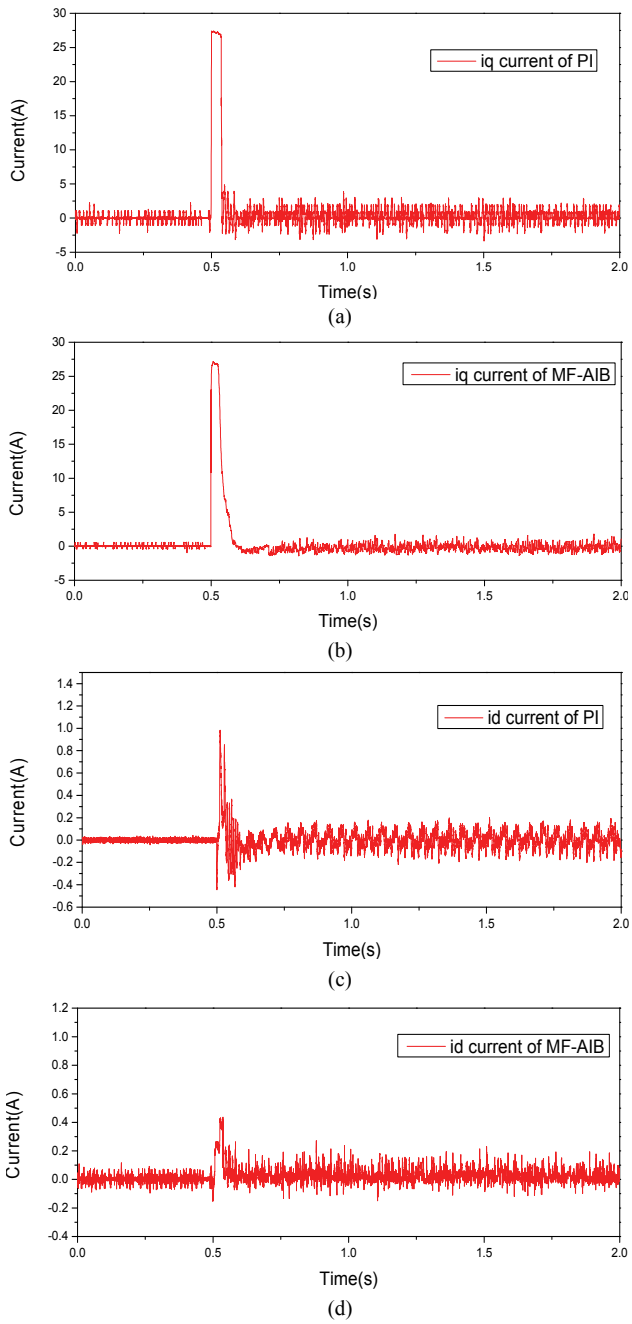

Fig. 7. Stator current comparison for the speed step response. (a) q-axis current response of a PI controller. (b) q-axis current response of the MF-AIB controller. (c) d-axis current response of a PI controller. (d) d-axis current response of the MF-AIB controller.

fully determined, and may contain some unknown objective factors. From Fig. 6, it can be seen that the motor driven by the MF-AIB has good speed performance. There is no steady-state error between the actual speed and the reference speed of the rotor, the convergence speed is fast and accurate, and the transient response does not have an overshoot. The good speed stepping performance of the MF-AIB controller is realized. Fig. 7 shows that the current fluctuation of the q-axis controlled by the MF-AIB is small and reaches a stable value

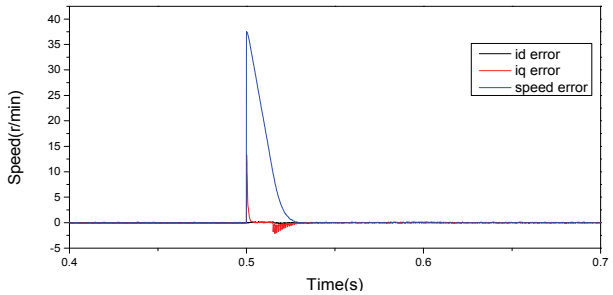

Fig. 8. Dynamic error characteristics of the proposed nonlinear controller.

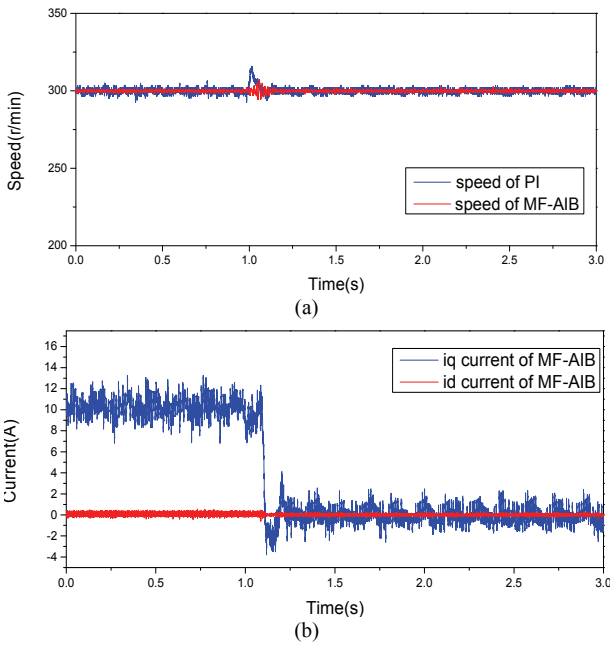

Fig. 9. Unloading performance at 300r/min speed. (a) Speed comparison between the MF-AIB control and PI control in an unloading experiment. (b) d-q axis current of the proposed controller in an unloading experiment.

quickly, while the impulse current of the d-axis is small when the speed is stepped.

The error curve shown in Fig. 8 is used to illustrate the steady-state stability and to show the amplitude of the current and velocity fluctuations. The error quickly converges to zero and enters a stable state, which verifies the Lyapunov stability of the proposed nonlinear controller.

In order to verify the dynamic response performance of the PMSM during a sudden unloading at medium speed, a speed control experiment of unloading at 300r/min was carried out. A load moment of 5N.m is applied to the PMSM driving bench, and the load torque is suddenly eliminated at 1s. Fig. 9 shows the rotor speed and current control performance. At the moment of unloading, the motor speed rises above the reference speed. The PI control results in a large deviation between the actual operation speed and the reference speed. As a comparison, the speed of the motor controlled by the MF-AIB only oscillates near the reference speed and quickly converges to the reference speed. These results clearly show that the MF-AIB has a stronger robustness and that the control algorithm has a stronger load disturbance rejection ability.

VII. Conclusion

This paper innovatively combines adaptive backstepping control with model-free control, and proposes a model-free adaptive integral backstepping (MF-AIB) control for SMPMSM driving systems. First, based on the input and output data of the system, three ultra-local models of the speed loop, d-axis current loop and q-axis current loop are established online. Meanwhile, with the help of the design idea of adaptive backstepping control, a matched adaptive backstepping integral controller is designed, which combines the speed closed-loop and the current closed-loop into a cascade structure. The basis for setting the parameters of the controller is given, and a concise model-free adaptive integral backstepping control structure for a SMPMSM driving system is constructed. The control scheme proposed in this paper can estimate and eliminate various uncertainties, including unmodeled dynamics and the "total" disturbances. When compared with PI control, it ensures the stability of the system, obtains better dynamic and steady-state control performance of the system and has strong robustness against load torque changes. It is expected to be widely applied in the electric drive systems of electric vehicles.

References

[1] X. Zhang, Y. He, and B. Hou, "Double vector based model predictive torque control for SPMSM drives with improved steady-state performance," *J. Power Electron.*, Vol. 18, No. 5, pp.1398-1408, Sep. 2018.

[2] A. Gaeta, G. Scelba, and A. Consoli, "Modeling and control of three-phase PMSMs under open-phase fault," *IEEE Trans. Ind. Appl.*, Vol. 49, No. 1, pp. 74-83, Feb. 2013.

[3] L. Sepulchre, M. Fadel, and M. Pietrzak-David, "Improvement of the digital control of a high speed PMSM for vehicle application," *2016 Eleventh International Conference on Ecological Vehicles and Renewable Energies (EVER)*, Monte Carlo, pp. 1-9, 2016.

[4] T. Kang, M.-S. Kim, and S. Y. Lee, "Modeling and a simple multiple model adaptive control of PMSM drive system ," *J. Power Electron.*, Vol. 17, No. 2, pp. 442-452, Mar. 2017.

[5] M. Ezzat, J. de Leon, and A. Glumineau, "Sensorless speed control of PMSM via adaptative interconnected observer," *Int. J. Contr.*, Vol. 84, No. 11, pp. 1926-1943, Nov. 2011.

[6] S. Alahakoon and T. Fernando, "Unknown input sliding mode functional observers with application to sensorless control of permanent magnet synchronous machines," *J. Franklin Inst.*, Vol. 350, No. 1, pp. 107-128, Feb. 2013.

[7] F. S. Del, D. Bruttomesso, and P. F. Di, "First use of model predictive control in outpatient wearable artificial pancreas," *Diabetes Care*, Vol. 37, No. 37, pp. 1212-1215, Jan. 2014.

[8] B. Z. Guo and Z. L. Zhao, "On the convergence of the nonlinear active disturbance rejection control for MIMO systems," *Contr. Optimization*, Vol. 51, No. 2, pp. 1727-1757, May 2013.
[9] J. Li, Y. Xia, and Z. Gao, "Study on the method of linear/nonlinear automatic disturb-restraint switching control," *Acta Automatica Sinica*, Vol. 42, No. 2, pp. 202-212, Mar. 2016.
[10] M. Fliess and C. Join, "Model-free control and intelligent PID controllers: Towards a possible trivialization of nonlinear control," *IFAC Proceedings Volumes*, Vol. 42, No. 10, pp. 1531-1550, Oct. 2015.
[11] Y. Zhou, H. Li, and H. Zhang, "Model-free deadbeat predictive current control of a surface-mounted permanent magnet synchronous motor drive system," *J. Power Electron*., Vol. 18, No. 1, pp. 103-115, Jan. 2018.
[12] Jesus R. Vazquez and A. D. Martin, "Backstepping control of a buck-boost converter in an experimental PV-system," *J. Power Electron.*, Vol. 15, No. 6, pp. 1584-1592, Nov. 2015.
[13] M. Karabacak and H. I. Eskikurt, "Design, modelling and simulation of a new nonlinear and full adaptive backstepping speed tracking controller for uncertain PMSM," *Applied Mathematical Modelling*, Vol. 36, No. 1, pp. 5199-5213, Jan. 2012.
[14] Y. Zhu, "Adaptive backstepping control for uncertain systems," *Ph.D. Thesis*, Zhejiang University, 2015.
[15] H. K. Khalil and P. V. Kokotovic, "On stability properties of nonlinear systems with slowly varying inputs," *IEEE Trans. Autom. Contr.*, Vol. 36, No. 2, pp. 229-241, Oct. 1991.
[16] H. P. Wang, Y. Tian, and N. Christov, "Piecewise-continuous observers for linear systems with sampled and delayed output," *Int. J. Syst. Sci.*, Vol. 47, No. 8, pp. 1804-1815, Aug. 2016.
[17] D. Tsubakino and M. Krstic, "Exact predictor feedbacks for multi-input LTI systems with distinct input delays," *Automatica*, Vol. 71, No. 7, pp. 143-150, Oct. 2016.
[18] Y. O. Lee, Y. Han, and C. C. Chung, "Output tracking control with enhanced damping of internal dynamics and its output boundedness for static synchronous compensator system," *IET Contr. Theory & Appl.*, Vol. 6, No. 10, pp. 1445-1455, Aug. 2012.
[19] S. Liu, X. Guo, and L. Zhang, "Robust adaptive backstepping sliding mode control for six-phase permanent magnet synchronous motor using recurrent wavelet Fuzzy Neural Network," *IEEE Trans. Autom. Contr.*, Vol. 1, No. 1, pp. 99-108, Jun. 2017.
[20] Y. H. Choi and S. J. Yoo, "Minimal-approximation based decentralized backstepping control of interconnected time-delay systems," *IEEE Trans. Cybernetics*, Vol. 46, No. 12, pp. 3401-3413, Oct 2016.
[21] X. Wang and C. Han, "A modified adaptive backstepping method for shaft deflection tracking control of magnetically suspended momentum wheel with nonlinear magnetic torque," *J. Franklin Inst.*, Vol. 99, No. 2, pp. 99-112, Mar. 2018.
[22] T. Ahmed-Ali and F. Giri, "Adaptive boundary observer for parabolic PDEs subject to domain and boundary parameter uncertainties," *Automatica*, Vol. 72, No. 2, pp. 115-122, Oct. 2016.
[23] B. M. Dehkordi, A. F. Payam, M. N. Hashemnia, and S.-K. Sul, "Design of an adaptive backstepping controller for doubly-fed induction machine drives," *J. Power Electron.*, Vol. 9, No. 3, pp. 343-353, May 2009.
[24] M. Fliess and C. Join, "Model-free control," *Int. J. Contr.*, Vol. 86, No. 12, pp. 2228-2252, Jul. 2013.
[25] M. Fliess and C. Join, "Stability margins and model-free control: A first look," in *IEEE European Control Conference*, pp. 454-459, 2014.
[26] H. J. Wang, M. Yang, L. Niu, and D. G. Xu, "Current-loop bandwidth expansion strategy for permanent magnet synchronous motor drives," *Proc. the 5th IEEE Conference on Industrial Electronics and Applications*, pp. 1340-1345, 2010.
[27] Y. C. Kwon, S. Kim, and S. K. Sul, "Voltage feedback current control scheme for improved transient performance of permanent magnet synchronous machine drives," *IEEE Trans. Ind. Electron.*, Vol. 59, No. 9, pp. 3373-3382, Sep. 2012.
[28] L. Harnefors, K. Pietiläinen, and L. Gertmar, "Torque-maximizing field-weakening control: Design, analysis, and parameter selection," *IEEE Trans. Ind. Electron.,* Vol. 48, No. 1, pp.161-168, Feb. 2001.
[29] Z. Gao, "Scaling and Bandwidth-Parameterization Based Controller Tuning," *Proc. American Control Conference*, 2003.
[30] M. Fliess and H. Sira-Ramírez, "Closed-loop parametric identification for continuous-time linear systems via new algebraic techniques," *Advances in Industrial Control*, pp. 363-391, 2008.

Hongmei Li was born in Anhui, China, in 1969. She received her B.S. and M.S. degrees in Electrical Engineering from the Hefei University of Technology, Hefei, China, in 1991 and 1996, respectively. She received her Ph.D. degree in Electrical Engineering from the Shenyang University of Technology, Shenyang, China, in 2003. She has been working as a Professor in the Department of Electrical Engineering, Hefei University of Technology, since 2006. Her current research interests include power electronics and motor control, predictive control, and the fault-tolerant control of electrical machine systems.

Xinyu Li was born in Shandong, China. He received his B.S. degree in Automation from Shandong University, Jinan, China, in 2002. He is presently working towards his Ph.D. degree in the Department of Electrical Engineering and Automation, Hefei University of Technology, Hefei, China. He is also working as a Lecturer in the Department of Mechanical and Electrical Engineering, Heze University, Heze, China. His current research interests include the ADRC control and robust control of electrical motor drives.

Zhiwei Chen was born in Anhui, China, 1988. He received his Ph.D. degree in Electrical Engineering from the Shenyang University of Technology, Shenyang, China, in 2017. He is presently working as a Lecturer in the School of Electrical and Automation Engineering, Hefei University of Technology, Hefei, China. His current research interests include engineering, electromagnetic fields, electromagnetic compatibility, and permanent magnetic medical actuators.

Jingkui Mao was born in Henan, China, in 1978. He is presently working towards his Ph.D. degree in the Department of Electrical Engineering and Automation, Hefei University of Technology, Hefei, China. He is also working an Associate Professor at the Henan Institute of Technology, Xinxiang, China. His current research interests include the predictive control and discrete space vector pulse width modulation of electrical motor drives.

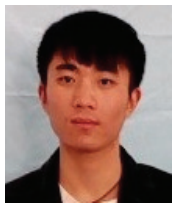

Jiandong Huang was born in Bengbu, China. He received his B.S. degree in Electronic Information Engineering from Hefei University, Hefei, China, in 2017, where he is presently working towards his Ph.D. degree in Electrical Engineering. His current research interests include the predictive control and robust control of electrical motor drives.